CHEMISTRY OF MATERIALS

ARTICLE

pubs.acs.org/cm

Realistic Modeling of Fluorescent Dye-Doped Silica Nanoparticles: A Step Toward the Understanding of their Enhanced Photophysical Properties.

Alfonso Pedone,*[,†] Giacomo Prampolini,[‡] Susanna Monti,[§] and Vincenzo Barone[‡]

[†]Dipartimento di Chimica, Università di Modena e Reggio Emilia, via G. Campi 183, 41125, Modena, Italia

[‡]Scuola Normale Superiore, Piazza dei Cavalieri 7, I-56126 Pisa, Italia

[§]Istituto di Chimica dei Composti Organo Metallici (ICCOM-CNR), Area della Ricerca, via G. Moruzzi 1, I-56124 Pisa, Italia

Supporting Information

ABSTRACT: The very high brightness and photostability of silica nanoparticles (NPs) encapsulating organic fluorophores have been demonstrated recently and have opened up new exciting opportunities for a number of biotechnological and information technological applications. However, a systematic theoretical study of fluorescent core−shell NPs remains a challenge, and as a result, the understanding of the fundamental interaction and microscopic dynamics of the dye/NPs assembly is still lacking. In the present work, different computational methods, as classical molecular dynamics simulations based on purposely tailored force-fields and TDDFT quantum mechanical calculations, are combined in an integrated strategy to elucidate the mechanisms behind the brightness enhancement of realistic models of rhodamine (TRITC) based C-dots (Cornell dots) for the first time. TD-B3LYP/MM calculations on the S_1 excited state dynamics of the dye show that crossing between the low lying (bright) $\pi\pi^*$ and (dark) $n\pi^*$ states occurs both in solution and in silica NPs albeit in the latter case it is reduced by the caging and screening effect played by the silica matrix. Moreover, our calculations show that the negligible solvatochromic shift between free-TRITC in solution and TRITC-based C-dots observed experimentally is because of seizure and incorporation of water molecules during the synthetic process that mediate the dye-silica interaction.

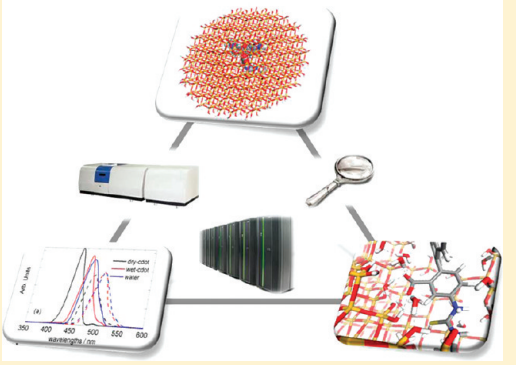

KEYWORDS: C-dot, silica, fluorophores, computational spectroscopy, TD-DFT, molecular dynamics

INTRODUCTION

Fluorescent nanoparticles (NPs) hold considerable promise for technological applications in biochemical, bioanalytical, and medical areas.[1,2] Current medical and biological fluorescent imaging methods are mainly based on dye markers, which have limited light emission per molecule, as well as photostability.[3] In the last decades, semiconductor quantum dots (Q dots) have emerged as possible bright and photostable substitutes, but because of their high price, toxicity, and difficult disposal, their use is sometimes impractical.[4]

Recently, it has been shown that an enhancement of fluorescence properties, such as quantum efficiency and particle brightness, can be obtained encapsulating covalently single or multiple dyes in silica-based materials and making small changes to the internal architecture of the formed particles.[5−7] More specifically, the effective building process leading to the formation of highly fluorescent monodisperse silica NPs, as described by Wiesner and co-workers,[8−10] consists essentially of two distinct phases, namely, the formation of a fluorophore-rich core inside a silica precursor and the addition of a siliceous shell to the system to protect the fluorescent core material from external perturbations, such as solvent interactions, which can affect negatively the photostability of the complex.

The examination of the photophysical characteristics of these complex systems at each stage of the synthesis, performed by means of fluorescence correlation spectroscopy (FCS),[11] revealed that the cores had a lower brightness in comparison with the core−shell particles and the free dyes. Conversely, the addition of a silica shell to the core significantly enhanced the brightness of the particles causing, at the same time, an increase in the radiative and a decrease in the nonradiative decay rates of the dye upon encapsulation. Beside the absence of any intermolecular quenching mechanisms, because of the lack of interactions between the dye and the surrounding solvent, silica caging effects, which reduce the mobility and flexibility of the encapsulated dye, could be another cause of C-dot enhanced brightness. This hypothesis originally stems from the findings obtained by incorporating multiple tetramethylrhodamine

Received: August 17, 2011
Revised: September 28, 2011
Published: October 19, 2011

isothiocyanate (TRITC) dye molecules into uniform monodisperse 25 nm diameter core−shell particles,[8] which provided a reduction of photobleaching kinetics of approximately an order of magnitude and gave brightness levels in solution similar to the ones shown by quantum dots of the same size.

Since then the behavior of multiple encapsulated-dyes from several families (Alexa fluor, courmarins, cyanines, perylenes, rhodamines, and fluorescein) that cover the entire UV−vis adsorption and emission spectrum have been investigated to create near-infrared fluorescent and large Stokes-shift fluorescent NPs for single excitation multiplexing.[9] Moreover, the coating of the silica surface with neutral and cationic polymers has been shown to facilitate efficient urinary excretion[12] and entrance to the cytoplasm,[13] which is very important for in vivo applications. Despite the wide use of inorganic matrices as shields between the solvent and the dyes, their radiative properties are not yet completely understood and are the subject of continued investigations.

For example, Wiesner and co-workers[10] suggested that the overall brightness enhancement of the particle, relative to the free dye, could be due to both the number of dye molecules inside the particle and to the relative quantum efficiency enhancement of the encapsulated dye.

Another class of dye-doped silica NPs were synthesized with a slightly different route by Prodi and colleagues[14] confirming that the number of dye molecules inside the particle is a fundamental factor affecting the final brightness.

Theoretical studies can provide valuable information on the photophysical and spectroscopic properties of fluorophores embedded into different chemical environments. In fact, their ability to simulate absorption and emission spectra of dye-doped NPs not only allows of interpretation of experimental results but also becomes fundamental to the design of new nanoarchitectures with improved performances. Accurate quantum mechanical (QM) calculations, based on Density Functional Theory (DFT) and its extensions to excited states (time-dependent DFT, TD-DFT)[15] have been used for the simulation of spectral properties of isolated dyes (in gas phase or in solution),[16−18] dimeric species,[19] and dyes adsorbed on inorganic surfaces,[20,21] but none of these studies dealt with dye-doped NPs.

Indeed, modeling the properties of NPs such as those designed by Wiesner's and Prodi's groups is very challenging from a computational point of view because of the difficulty of coupling the accuracy of the calculations with the system dimensions.

At present *ab initio* MD simulations cannot be employed on excited states of for systems containing more than hundreds of atoms and for periods longer than hundreds of picoseconds while the excited state lifetimes of the dye molecules commonly employed in the bioimaging field are of the order of nanoseconds. The temporal and spatial scale can be expanded by employing low level semiempirical method, but at the price of reducing the reliability of the calculations.

For this reason, we have adopted a new computational multilevel approach, that integrates classical molecular dynamics (MD) simulations with accurate QM-tailored force-fields and mixed quantum-mechanical/molecular mechanical (QM/MM) methods.[22,23]

Therefore, a delicate and important step required for succeed in the simulation of dye-doped NPs is the development of sophisticated classical force-fields which reproduce the QM potential energy surface of both the ground and the excited state of the dye-silica assemblies.[24]

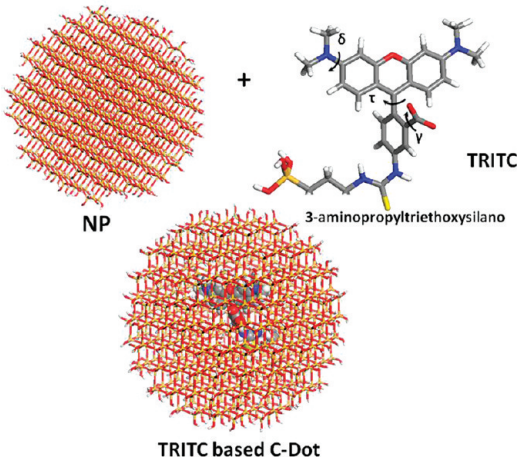

Figure 1. Structural model of the TRITC based C-dot generated and subsequently used throughout the manuscript. Red, gray, blue, yellow, and white spheres represent oxygen, carbon, nitrogen, sulfur, and hydrogen atoms of the organic dye, respectively. Red and yellow sticks represents oxygen and silicon atoms of the silica NP.

In this work, this multilevel approach is applied to the study of the conformational flexibility, spectroscopic, and photophysical properties of rhodamine (TRITC) based C-dots. Our aim is to describe the physicochemical properties of these assemblies, which have not been theoretically investigated to date, through realistic models and to explain how these properties are influenced by the surrounding environment, being it mere solvent or a complex supramolecular system.

COMPUTATIONAL DETAILS

As a first step of our approach, we used classical MD simulations to investigate the dynamics and the structural properties of the ground (S_0) and excited (S_1) states of the TRITC based C-dot model displayed in Figure 1. A nanoparticle of 42 Å diameter with structural characteristics similar to a silica glass,[25] was cut out from a 8 × 8 × 8 cubic supercell of relaxed β-cristobalite and saturated with hydroxyl groups. Subsequently, the TRITC molecule conjugated to 3-aminopropyltriethoxysilane was covalently bound to the −OH terminated walls of the particle hosting cavity.

Our structural model containing a single dye molecule could represent with good accuracy experimentally tailored homogeneous particles produced by the Wiesner group[10] containing sparse dyes and showing a more pronounced decrease in the nonradiative decay rate.[10]

That is, in NPs where the formation of dimeric species is avoided or at least reduced. This is not always true as demonstrated by several papers from the Prodi's group where the fluorescence quenching between dimeric species into the silica matrix were investigated.[26] A different model should be created to study the interesting behavior of two molecules inside the particle, a topic that will be covered in future works.

Since it is likely that during the synthesis of these NPs a small amount of water molecules could remain trapped, along with the dye, inside the nanoparticle cavity, we increased further the complexity of our prototype, to take into account this effect, and defined another model where the cavity contained not only the dye but also a few (24) water molecules.

This is the number of water molecules able to fill the empty space into the hosting cavity without creating overlaps with other molecules.

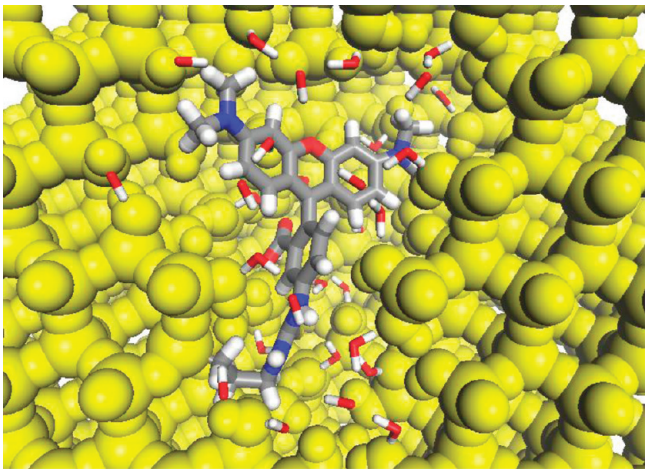

Figure 2. Perspective view of the hosting cavity of the wet C-dot containing the dye and 24 water molecules. The yellow spheres represent the atoms of the silica shell. The TRITC molecule is bonded to the silica shell through a Si−C bond.

A partial view of the cavity for the structural model of the core−shell NP containing the dye and the 24 water molecules which highlights the chemical bond between the dye and the silica shell is reported in Figure 2.

From now on we will refer to the first system as dry C-dot and to the second system as wet C-dot.

All MD simulations were performed with the GULP code[27] by using accurately tuned force fields and effective simulation protocols.[18,28] In particular, the intra-molecular force-fields of both the ground and excited states of TRITC were derived through the Joyce[24] parameterization procedure, which was based on B3LYP and TD-B3LYP calculations with purposely tailored basis set,[18,28] whereas a self-consistent rigid-ionic pairwise interatomic potential, developed by Pedone et al.[29] was used for the silica shell.

Whereas the dyes FF's have been successfully employed to simulate the conformational flexibility and spectroscopic UV−vis parameters such as solvatochromic shifts and Stokes shift of the free molecule in solution,[18,28] the latter one was parameterized on the experimental structure and elastic constants of oxides and silicates[29,30] and validated in a number of papers dealing with the simulation of the structure, transport, and mechanical properties of silica based glasses.[31−34]

A Buckingham potential was used to describe the interaction between the hydrogen atoms (Ho) of the hydroxyl groups at the silica surfaces and the oxygen atoms (Oc) of the carboxylate group of the TRITC molecule. The relative parameters were fitted by reproducing the binding energy and the optimized structure of TRITC molecules adsorbed onto silica surfaces.[35] The remaining intermolecular interactions were modeled by a using Lennard-Jones potentials whose parameters were taken from the OPLS force field available in literature.[36−38]

Full details on the force-field parameters and the calculations performed in the present work are given in the Supporting Information.

After a full geometry optimization of the whole models, MD simulations in the ground state have been carried out by allowing both TRITC and the first shell of SiO_4 tetrahedra (and the water molecules inside the cavity for the wet C-dot system) surrounding it to move freely, whereas the rest of the system was kept fixed at the atomic positions previously relaxed. The excited state trajectory was generated starting from the last snapshot of the ground state dynamics so as to mimic the light absorption within the Franck−Condon approximation.

As better explained in the Supporting Information the UV−vis absorption and emission spectra were simulated employing 100 frames randomly extracted from the above-mentioned S_0 and S_1 classical MD simulations.

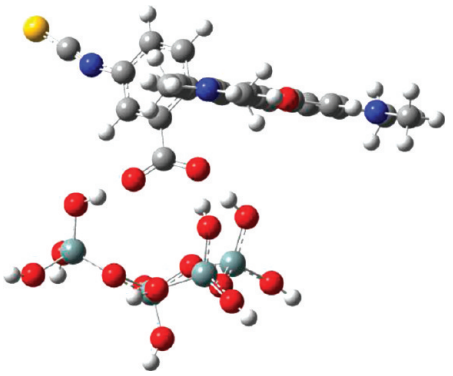

Figure 3. TRITC/silica assembly optimized at the B3LYP/N07D level and used to fit the Ho−Oc interatomic potential parameters.

For each frame the peak positions and oscillator strengths of the absorption $S_1 \leftarrow S_0$ and emission $S_1 \rightarrow S_0$ transitions were calculated by using TD-DFT(B3LYP)/MM simulations, broadened with Gaussian functions and coadded to yield the final spectrum.

$$\varepsilon(\lambda) = \sum_{i=1}^{N} \frac{f_i}{\sigma} \exp\left(-2.773 \frac{(\lambda - \lambda_i)^2}{\sigma^2} \right)$$

where f_i is the oscillator strength of the i-th transition, N is the number of transitions (here one because we studied the $S_1 \leftarrow S_0$ and $S_1 \rightarrow S_0$ transitions for the absorption and emission spectra, respectively), λ_i is the wavelength of electronic transitions energies in nm and σ is the half-bandwidth which has been taken equal to 15 nm.

To take into account the effects due to the electronic reorganization of the surrounding environment on the new electronic distribution of the dye during the electronic transition, the molecules directly coordinated to the carboxyl group (water or silica tetrahedra) have been included into the quantum mechanical description (together with the TRITC molecule) while the rest of the system has been treated through force field parameters within the ONIOM electronic embedding scheme. All the TDDFT/MM calculations have been carried out by means of the Gaussian09 code.[39]

RESULTS AND DISCUSSIONS

Development of the FF Parameters for the TRITC−Silica Interaction. In a recent work, the interaction between the TRITC molecule and silica surfaces has been investigated by adsorbing the fluorophore on a realistic model of amorphous silica surface and performing QM/MM calculations to study the structural, energetic, and electronic features of the TRITC-silica assembly.[35]

The structural properties and the binding energies of the TRITC/silica assembly reported in Figure 3 have been computed at the B3LYP/N07D level of theory and then employed to fit interatomic potential parameters between the carboxylate group of the dye and the silanols group at the silica surface.

As described in the Computational Details, this interaction has been modeled by employing a Buckingham function whose parameters are reported in Table 6 of the Supporting Information.

A first validation of the proposed FF was obtained by performing an MM minimization on the TRITC molecule adsorbed on the silica slab. The comparison between the most relevant internal coordinates optimized at the QM and MM levels as well as the binding energies (reported in Table 1), shows that the two sets are in remarkable agreement.

Table 1. Structural, Energetic Parameters and Vertical Transition Energies Calculated on the S_0 and S_1 Geometry of the TRITC/Silica Assembly (see Figure 3) Optimized with the B3LYP/N07D and at the Molecular Mechanics Level of Theory

	QM(S_0)	MM(S_0)	QM(S_1)	MM(S_1)
d_{Hb1} (Å)	1.650	1.658	1.633	1.666
d_{Hb2} (Å)	1.747	1.740	1.715	1.659
d_{Hb3} (Å)	1.652	1.711	1.649	1.627
τ (deg)	81.2	82.7	62.1	63.5
γ (deg)	15.7	14.0	28.9	43.4
θ (deg)	124.7	125.8	124.4	122.6
$E_{binding}$ (eV)	−1.22	−1.20	−1.25	−1.24
VE($S_1 \leftarrow S_0$) (nm)	474.1 (0.9)	475.9 (0.9)		
VE($S_1 \rightarrow S_0$) (nm)			504.2 (0.78)	506.3 (0.80)

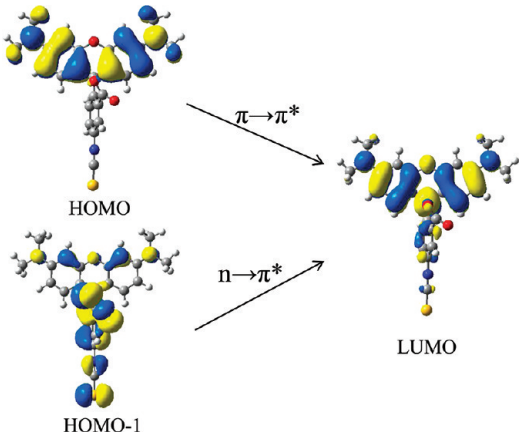

Figure 4. Shape of the Khon−Sham orbitals involved in the $\pi \rightarrow \pi^*$ (HOMO → LUMO) and $n \rightarrow \pi^*$ (HOMO−1 → LUMO) transitions.

Finally, the optimized S_0 and S_1 MM geometry has been used to calculate the vertical $S_1 \leftarrow S_0$ and $S_1 \rightarrow S_0$ transition energies at the QM level, accounting for bulk solvent effects at PCM level.[40] The $S_1 \leftarrow S_0$ and the $S_1 \rightarrow S_0$ transition energies of 475.9 and 506.3 nm compare fairly well with the one calculated using the structure optimized at the QM level.

Therefore, these results show that the new FF seems robust enough to be employed in MD simulations to study dynamical effects and the structural properties of the TRITC molecule in the silica NPs.

Molecular Dynamics and Photophysical Properties of TRITC-Based C-Dots. Earlier studies, focusing on the photophysical properties of the TRITC molecule in solution,[16,17,41] have revealed that this molecule has two low lying excited states, namely S_1 and S_2, with ($\pi\pi^*$) and ($n\pi^*$) character, respectively. S_1 is a bright state given by the transition between the HOMO −LUMO Kohn−Sham orbitals, while S_2 is a dark state involving the HOMO−1 and LUMO orbitals reported in Figure 4.

Our calculations showed that the new functional groups of the conjugated dye have no effect either on the enhancement of the dye brightness or on the $\pi\pi^*$ excited state in agreement with previous experimental findings,[42] whereas the molecular orbitals localized on the carboxylate group and on the xanthenes moiety are more influenced by the surrounding environment.[35]

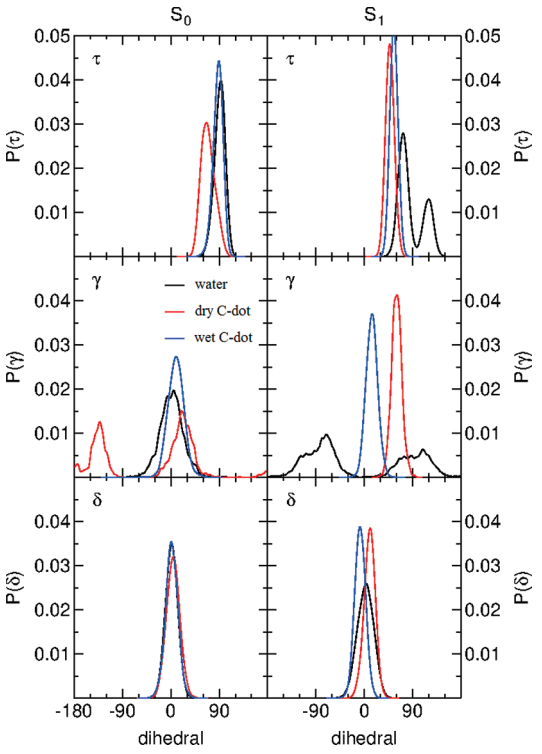

Figure 5. Probability distribution functions of the δ, τ, and γ dihedral angles of free-TRITC in water solution (black lines), dry C-dot (red lines), and wet C-dot (blue lines) for both the ground and the $\pi\pi^*$ excited states.

According to the extensive literature, which describes the effects of various environmental quenchers (oxygen, solvent relaxation, etc.) that decrease both the steady state fluorescence emission intensity and the excited state lifetime by merely increasing the nonradiative decay rate, internal rotations often provide additional channels for nonradiative de-excitation. In this respect, the conformational flexibility of the TRITC molecule in C-dot has been investigated by analyzing the probability distribution functions of the flexible dihedral angles δ, τ, and γ shown in Figure 1, and comparing them with those extracted from the dynamics of the molecule in water solution.[18,28]

The ground and the $\pi\pi^*$ excited state probability distribution functions of the aforementioned dihedral angles of TRITC free in water and bound in the NPs (TRITC-based C-dot) are shown in Figure 5.

As it can be observed, while τ distributions in water are quite different in the ground and excited states, they are very similar when TRITC is embedded into the dry NP and shifted when trapped water molecules are present.

As expected, the distributions of all the torsion angles are broader in water than in the NPs, but the encapsulation effect is more pronounced for the excited state, which becomes more rigid both in the xanthenes and carboxyl portions of the molecule. This is confirmed by the remarkable decrease in both τ and γ distribution widths and by the disappearance of double peaks present in solution. On the contrary, the overall conformation of the ground state appears less affected by the silica cage. However, also in this case peak values are shifted and the rotation of the carboxyl group, not surrounded by water molecules, becomes wider and biased by the location and motion of the nearby OH moieties of the NP surface.

dx.doi.org/10.1021/cm202436b |*Chem. Mater.* 2011, 23, 5016–5023

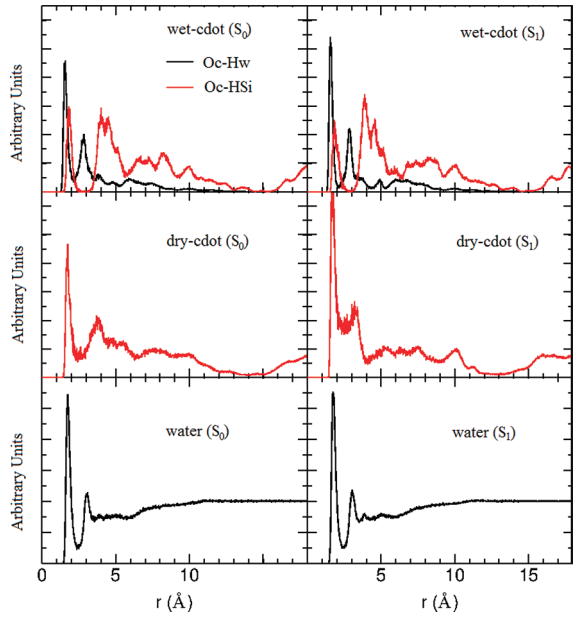

Figure 6. Radial distribution functions between the oxygen atoms of the carboxylate group (Oc) and the hydrogen atoms of silica (HSi) and water (Hw) for both the ground and excited states dynamics of the TRITC molecule in wet C-dot, dry C-dot, and water solution.

The most stable conformation of the ground state in water is the one where τ and γ are centered at about 93 and 0°, respectively, while in the excited state the molecule explores four different conformations.[18,28]

As for the τ and δ dihedral angles distributions in C-dots, our results show that they are similar for both the ground and the excited states, in the latter case the molecule assumes only one configuration where τ and γ are centered at about 60 and 0° for wet C-dot and at about 60° and 50° for dry C-dot, respectively. The single peaked distribution found for the γ angle in the excited state confirms that the silica-TRITC interaction in the dry NP or the silica-water-TRITC interaction into the wet NP is stronger in the excited state than in the ground state were this angle can assumes two conformations. Instead, δ remains close to 0° in all cases.

These data suggest that after absorption of light the silica shell interferes with the rotation of the torsion angles hampering the geometric relaxation that occur in water solution after excitation.

The rigidity of the silica shell can also be envisaged by analyzing the radial distribution functions between the oxygen atoms (Oc) of the carboxylate group and the hydrogen atoms (HSi and Hw) of the silanol groups and water molecules for the TRITC-based C-dot models and free-TRITC in their ground and excited states.

The RDFs (Figure 6) show a first peak at about 1.8 Å for both S_0 and S_1 in agreement with the fact that the negative charge on the carboxyl oxygens (Oc) is similar in the two states and that the TRITC molecule strongly interacts with both the silica shell and water molecules essentially through these atoms. However, the distributions computed for the molecule embedded into the dry and wet NPs are narrower than those found in water. This is a consequence of the rigidity of the surrounding environment, which prevents major conformational changes of the dye. The carboxyl moiety of TRITC in the dry-NP is coordinated by two hydroxyl groups during the whole simulation time, whereas in water solution it is surrounded by 4−5 water molecules.

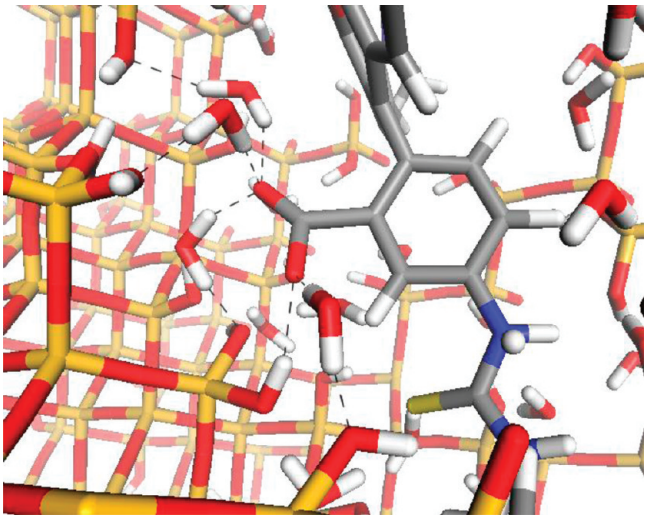

Figure 7. Hydrogen bond network formed by the water molecules interposed between the TRITC molecule and the silica shell.

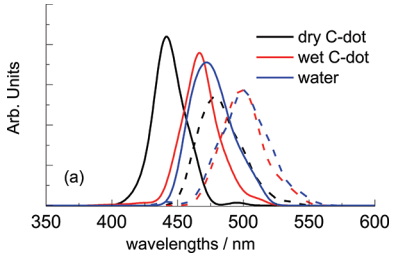

Figure 8. Absorption (solid lines) and emission (dashed lines) spectra of the TRITC molecule embedded into a dry C-dot (black lines), a wet C-dot (red lines), and in water solution (blue lines).

It is interesting to note the role played by the water molecules included into the hosting cavity of the wet C-dot.

During the MD equilibration phase, five water molecules move toward the carboxylate group mediating the interaction between the silica shell and TRITC through the formation of a network of strong hydrogen bonds as shown in Figure 7. These molecules are not able to exchange with a second coordination sphere as it happens in water and they remain coordinated to the carboxylate group also in the excited state.

In Figure 8, the absorption and emission spectra of the dry and wet C-dot models are compared to the ones of free-TRITC in water.

In both cases, the simulated absorption and emission spectra are shifted by about 80 nm with respect to the experimental data, a discrepancy which has already been reported for rhodamine derivatives in several computational works.[17,19,20,43]

The peaks of the absorption spectra of the dry C-dot and free-TRITC lie at around 443 and 470 nm, respectively, and they show a 27 nm solvatochromic shift in contrast with the negligible shift issuing from experimental evidence.[8]

A similar solvatochromic shift is seen also in the emission spectra, whose maxima lie at around 478 and 500 nm for dry C-dot and free-TRITC, respectively.

Interestingly, the solvatochromic shift almost disappears for the wet C-dot model demonstrating that the five water molecules interposed between the carboxylate group and the silica shell play

dx.doi.org/10.1021/cm202436b |*Chem. Mater.* 2011, 23, 5016–5023

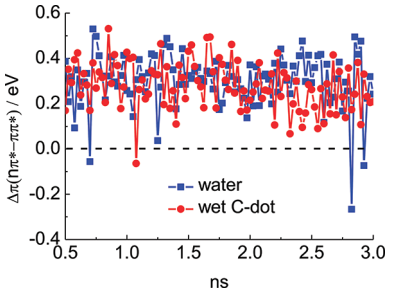

Figure 9. Time evolution of the energy difference between the (nπ^*) and ($\pi\pi^*$) excited states along the ($\pi\pi^*$) trajectories of the TRITC molecule in solution (blue line) and embedded into wet C-dot (red line).

a major effect on the UV−vis spectra. Therefore, our results suggest that during the synthesis of dye-doped NPs a few water molecules remain trapped into the cavity. This fact was never discussed in previous experimental works and in our opinion it should be better investigated in future experiments.

A fair agreement is also obtained in reproducing the experimental Stoke shift, which is about 25 nm. In fact the calculated Stokes shift of free-TRITC in water solution is around 30 nm while that computed for the wet C-dot is around 33 nm.

Finally, the UV−vis spectra of both the C-dot models are slightly narrower than the ones of free-TRITC in water, in agreement with the reduced mobility already demonstrated by analyzing the MD trajectories.

The results of this investigation confirm the experimental hypothesis that the decreasing of the nonradiative decay rate of the dye embedded into the NP might be due to a constraining action that the NP performs on TRITC geometry (caging effect) which could avoids intramolecular channels of nonradiative decay, thus enhancing device brightness.

To corroborate this hypothesis we have analyzed the ($\pi\pi^*$) and (nπ^*) low lying excited states through TDDFT/MM calculations on one hundred configurations randomly extracted from the ($\pi\pi^*$) excited state dynamics of free-TRITC in water and into the wet C-dot.

Figure 9 shows the time evolution of the energy difference between the (nπ^*) and ($\pi\pi^*$) states along the excited state trajectory for free-TRITC and wet C-dot, respectively. From the figure it can be inferred that the adiabatic energies of the ($\pi\pi^*$) and (nπ^*) states in water solution are very close to each other during the entire simulation and, in three cases, the (nπ^*) state happens to lie at a lower energy with respect to the ($\pi\pi^*$) state (when the difference between the two states is negative). This suggests that a competition between a bright and a dark state, whose average energy gap is around 0.3 eV, can lead to a quenching of fluorescence thanks to the nonradiative decay through crossing points of the two potential energy surfaces. In fact, about 3% of the snapshots, extracted from the MD simulations performed in water, present intersection points between these two states. Instead, only one crossing point is detected when the fluorophore is encapsulated in the wet C-dot and in this case the TDDFT calculations show that there is a mixing between the pure (nπ^*) and ($\pi\pi^*$) states which results in two low-lying bright states.

Recently, Larson et al.[10] determined the quantum yield of TRITC molecules encapsulated into NPs with different internal architectures. They stated that the measured brightness of the silica NPs is due both to the incorporation of multiple dye molecules and to enhancement of the quantum efficiency of the incorporated dye molecules.

The latter was ascribed to a uniform 2-fold increase of the radiative rate (independent of the NP architecture) and a variable reduction of the nonradiative rate (up to a factor of 3 for homogeneous particle with dye molecules sparsely embedded within) which varied inversely with the degree of rotational mobility of the dye allowed by the architecture.

Instead, Prodi and co-workers[44] argued that the high brightness of the NP, which is defined as the product of the molar absorption coefficient and the fluorescent quantum yield,[45] is due to the presence of a large number of absorbing moieties in a single NP.

However, it is worth noticing that they use different synthetic procedures and that the architecture of their NPs are different with respect to that produced by the Wiesner group.

In fact, Prodi and colleagues have also investigated the energy transfer occurring between different dyes present into the NPs or the fluorescent quenching between similar dyes into the silica matrix, a fact that demonstrate that a high amount of dimeric species might be present into some of their NPs.

This interesting topic was not covered in the present paper which confirm the caging effect played by the silica shell to the dye mobility in good agreement with the experimental findings reported by Wiesner and coworkers.[10]

Our results show that the energy gap between the ground and the first ($\pi\pi^*$) excited state is quite large (2.3−2.8 eV) during the whole trajectory and thus a de-excitation involving the nπ^* excited state is possible. Albeit, the crossing between the bright ($\pi\pi^*$) and the dark (nπ^*) excited states is reduced into the NPs the very similar energy gap between the two states in both water solution as well as into the wet-NP cannot rule out a partial ($\pi\pi^*$) → (nπ^*) population transfer even into the NP. A quantitative investigation of the nonradiative rate and thus the mechanism of de-excitation would require the computation of the nonadiabatic coupling between these three states along the ground and excited state dynamics. However, we have not yet implemented such a calculation in our general tool and it will be the subject of future efforts.

CONCLUSIONS

In conclusion, on the basis of accurate MD simulations and TDDFT/MM calculations, we have provided a detailed characterization of the electronic structure as well as the absorption and emission spectra of possible models of rhodamine (TRITC) based C-dots. To the best of our knowledge, this is the first work in which a multiscale computational approach is used to investigate the electronic and dynamic effects which lead to increased fluorescence quantum yield of fluorophores encapsulated in silica NPs.

It is worth noticing that an accurate calculation of the absorption and fluorescence spectra with respect to its experimental counterpart depends on the quality of the MD simulations, hence on the reliability of the employed force field (FF). To this end, a careful parametrization of the ground (S_0) and the first bright excited state (S_1) is necessary as well as the development of reliable force-field for the investigation of the TRITC-silica interaction. Despite there being a lot of FF parametrizations for the ground state geometries of organic molecules,[46] this is the first one that involves all internal degrees of freedom of an excited state simultaneously. Moreover, also in the case of the simulation

of the absorption spectra, the transition energies are so strongly dependent on the S_0 geometry that standard classical force-fields reported in literature can yield misleading results.

TDDFT/MM calculations on the dye-doped NPs studied in this work show that crossing between the low-lying (bright) $\pi\pi^*$ and (dark) $n\pi^*$ states occurring in solution is reduced by the more rigid environment offered by the silica shell. As for the negligible solvatochromic shift observed experimentally between free-TRITC in water solution and TRITC-based C-dots, our results indicate that this is imputable to a few water molecules, which remain entrapped into the silica NPs during their synthesis. These molecules form a strong hydrogen bond network, which mediates the TRITC-silica interaction leading to UV−vis spectra very similar to that observed in water solution.

Finally, the conceptual simplicity of the theoretical foundation of the approach proposed in this paper leads to a procedure easily accessible to not specialists and fully transferable to investigate the photophysical properties of different families of dye-doped NPs, which are of particular technological interest for a large variety of interesting applications.

■ ASSOCIATED CONTENT

Supporting Information. Full details on the force-field parameters and the calculations performed in the present work. This material is available free of charge via the Internet at http://pubs.acs.org.

■ AUTHOR INFORMATION

Corresponding Author
*E-mail: alfonso.pedone@unimo.it.

■ ACKNOWLEDGMENT

A.P. thanks "Telecom Italia" for financial support through grants and Dr. Marco Montalti (University of Bologna, Italy) for fruitful discussions.

■ REFERENCES

(1) Jaiswal, J. K.; Mattoussi, H.; Mauro, J. M.; Simon, S. M. *Nat. Biotechnol.* **2003**, *21*, 47.
(2) Goldman, E. R.; Clapp, A. R.; Anderson, G. P.; Uyeda, H. T.; Mauso, J. M.; Medintz, I. L.; Mattoussi, H. *Anal. Chem.* **2004**, *76*, 684.
(3) Haugland, R. P. The Handbook. *A Guide to Fluorescent Probes and Labeling Technologies*, 10th ed.; Molecular Probes, Inc.: Eugene, OR, 2005.
(4) Derfus, A. M.; Chan, W. C. W.; Bathia, S. N. *Nano Lett.* **2004**, *4*, 11.
(5) Nguyen, N. N.; Smit, M.; Dunn, B.; Zink, J. I. *Chem. Mater.* **2002**, *14*, 4300.
(6) Jin, W.; Brennan, J. D. *Anal. Chem. Acta* **2002**, *461*, 1.
(7) Gilliland, J. W.; Yokoyama, K.; Yip, W. T. *Chem. Mater.* **2005**, *17*, 6702.
(8) Ow, H.; Larson, S. M.; Srivastava, M.; Baird, B. A.; Webb, W. W.; Wiesner, U. *Nano Lett.* **2005**, *5*, 113.
(9) Burns, A.; Ow, H.; Wiesner, U. *Chem. Soc. Rev.* **2006**, *35*, 1028.
(10) Larson, S. M.; Ow, H.; Vishwasrao, H. D.; Heikal, A. A.; Wiesner, U.; Webb, W. W. *Chem. Mater.* **2008**, *20*, 2677.
(11) Hess, S. T.; Huang, S.; Heikal, A. A.; Webb, W. W. *Biochemistry* **2002**, *41*, 697.
(12) Burns, A.; Vider, J.; Ow, H.; Herz, E.; Penate-Medina, O.; Baugmgart, M.; Larson, S. M.; Wiesner, U.; Bradbury, M. *Nano Lett.* **2009**, *9*, 442.
(13) Fuller, J. E.; Zugates, G. T.; Ferreira, L. S.; Ow, H. S.; Nguyen, N. N.; Wiesner, U. B.; Langer, R. S. *Biomaterials* **2008**, *29*, 1526.
(14) Bonacchi, S.; Genovese, D.; Juris, R.; Montalti, M.; Prodi, L.; Rampazzo, E.; Zaccheroni, N. *Angew. Chem., Int. Ed.* **2011**, *50*, 4056.
(15) Dreuw, A.; Head-Gordon, M. *Chem. Rev.* **2005**, *105*, 4009.
(16) Pedone, A.; Barone, V. *Phys. Chem. Chem. Phys.* **2010**, *12*, 2722.
(17) Pedone, A.; Bloino, J.; Monti, S.; Prampolini, G.; Barone, V. *Phys. Chem. Chem. Phys.* **2010**, *12*, 1000.
(18) Barone, V.; Bloino, J.; Monti, S.; Pedone, A.; Prampolini, G. *Phys. Chem. Chem. Phys.* **2010**, *12*, 10550.
(19) Setiawan, D.; Kazaryan, A.; Martoprawiro, M. A.; Filatov, M. *Phys. Chem. Chem. Phys.* **2010**, *12*, 11238.
(20) Labat, F.; Ciofini, I.; Hratchian, H. P.; Frisch, M. J.; Raghavachari, K.; Adamo, C. *J. Am. Chem. Soc.* **2009**, *131*, 14290.
(21) De Angelis, F.; Tilocca, A.; Selloni, A. *J. Am. Chem. Soc.* **2004**, *126*, 15024.
(22) Maseras, F.; Morokuma, K. *J. Phys. Chem.* **1995**, *100*, 19357.
(23) Svensson, M.; Humbel, S.; Froese, R. D. J.; Matsubara, T.; Sieber, S.; Morokuma, K. *J. Phys. Chem.* **1996**, *100*, 19357.
(24) Cacelli, I.; Prampolini, G. *J. Chem. Theory Comput.* **2007**, *3*, 1803.
(25) Chang, E.; Thekkek, N.; Yu, W. W.; Colvin, V. L.; Drezek, R. *Small* **2006**, *2*, 1412.
(26) Montalti, M.; Prodi, L.; Zaccheroni, N.; Zattoni, A.; Reschiglian, P.; Falini, G. *Langmuir* **2004**, *20*, 2989.
(27) Gale, J. D.; Rohl, A. L. *Mol. Simul.* **2003**, *29*, 291.
(28) Barone, V.; Bloino, J.; Monti, S.; Pedone, A.; Prampolini, G. *Phys. Chem. Chem. Phys.* **2011**, *13*, 2160.
(29) Pedone, A.; Malavasi, G.; Menziani, M. C.; Cormack, A. N.; Segre, U. *J. Phys. Chem. B* **2006**, *110*, 11780.
(30) Pedone, A. *J. Phys. Chem. C* **2009**, *113*, 20773.
(31) Pedone, A.; Malavasi, G.; Cormack, A. N.; Segre, U.; Menziani, M. C. *Chem. Mater.* **2007**, *19*, 3144.
(32) Pedone, A.; Malavasi, G.; Cormack, A. N.; Segre, U.; Menziani, M. C. *Theor. Chem. Acc.* **2008**, *120*, 557.
(33) Pedone, A.; Malavasi, G.; Menziani, M. C.; Segre, U.; Cormack, A. N. *J. Phys. Chem. C* **2008**, *112*, 11034.
(34) Pedone, A.; Malavasi, G.; Menziani, M. C.; Segre, U.; Cormack, A. N. *Chem. Mater.* **2008**, *20*, 4356.
(35) Pedone, A.; Prampolini, G.; Monti, S.; Barone, V. *Phys. Chem. Chem. Phys.* **2011**, *13*, 16689.
(36) McDonald, N.; Jongersen, W. *J. Phys. Chem. B* **1998**, *102*, 8049.
(37) Price, M.; Ostrowsky, D.; Jongersen, W. *J. Comput. Chem.* **2001**, *22*, 1340.
(38) Wensink, E. J. W.; Hoffmann, A. C.; Apol, M. E. F.; Berendsen, H. J. C. *Langmuir* **2000**, *16*, 7392.
(39) Frisch, M. J. T., G. W.; Schlegel, H. B.; Scuseria, G. E.; Robb, M. A.; Cheeseman, J. R.; Scalmani, G.; Barone, V.; Mennucci, B.; Petersson, G. A.; Nakatsuji, H.; Caricato, M.; Li, X.; Hratchian, H. P.; Izmaylov, A. F.; Bloino, J.; Zheng, G.; Sonnenberg, J. L.; Hada, M.; Ehara, M.; Toyota, K.; Fukuda, R.; Hasegawa, J.; Ishida, M.; Nakajima, T.; Honda, Y.; Kitao, O.; Nakai, H.; Vreven, T.; Montgomery, Jr., J. A.; Peralta, J. E.; Ogliaro, F.; Bearpark, M.; Heyd, J. J.; Brothers, E.; Kudin, K. N.; Staroverov, V. N.; Kobayashi, R.; Normand, J.; Raghavachari, K.; Rendell, A.; Burant, J. C.; Iyengar, S. S.; Tomasi, J.; Cossi, M.; Rega, N.; Millam, N. J.; Klene, M.; Knox, J. E.; Cross, J. B.; Bakken, V.; Adamo, C.; Jaramillo, J.; Gomperts, R.; Stratmann, R. E.; Yazyev, O.; Austin, A. J.; Cammi, R.; Pomelli, C.; Ochterski, J. W.; Martin, R. L.; Morokuma, K.; Zakrzewski, V. G.; Voth, G. A.; Salvador, P.; Dannenberg, J. J.; Dapprich, S.; Daniels, A. D.; Farkas, Ö.; Foresman, J. B.; Ortiz, J. V.; Cioslowski, J.; Fox, D. J. *Gaussian*; revision A.1 ed.; Gaussian, Inc.: Wallingford CT, 2009.
(40) Tomasi, J.; Mennucci, B.; Cammi, R. *Chem. Rev.* **2005**, *105*, 2999.
(41) Pedone, A.; Biczysko, M.; Barone, V. *ChemPhysChem* **2010**, *11*, 1812.
(42) Herz, E.; Ow, H.; Bonner, D.; Burns, A.; Wiesner, U. *J. Mater. Chem.* **2009**, *19*, 6342.

(43) Hazebroucq, S.; Labat, F.; Lincot, D.; Adamo, C. *J. Phys. Chem. A* **2008**, *112*, 7264.
(44) Rampazzo, E.; Bonacchi, S.; Juris, R.; Montalti, M.; Genovese, D.; Zaccheroni, N.; Prodi, L.; Rambaldi, D. C.; Zattoni, A.; Reschiglian, P. *J. Phys. Chem. B* **2010**, *114*, 14605.
(45) Braslavsky, S. E. *Pure Appl. Chem.* **2007**, *79*, 293.
(46) Cornell, W. D.; Cieplak, P.; Bayly, C. I.; Gould, I. R.; Merz, K. M. J.; Ferguson, D. M.; Sellmeyer, D. C.; Fox, T.; Caldwell, J. W.; Kollman, P. A. *J. Am. Chem. Soc.* **1995**, *117*, 5179.